Inorganic Chemistry

Article

pubs.acs.org/IC

Interplay between Local Anisotropies in Binuclear Complexes

Renaud Ruamps,[†] Rémi Maurice,[‡] Coen de Graaf,[¶,§] and Nathalie Guihéry*[,†]

[†]Laboratoire de Chimie et de Physique Quantiques, IRSAMC/UMR5626, Université de Toulouse 3, 118 route de Narbonne, F-31062 Toulouse Cédex 4, France

[‡]SUBATECH, UMR CNRS 6457, IN2P3/EMN Nantes/Université de Nantes, 4 rue Alfred Kastler BP 20722, 44307 Nantes Cédex 3, France

[¶]Departament de Química Física i Inorgànica, Universitat Rovira i Virgili, Marcel·lí Domingo s/n, 43007 Tarragona, Spain

[§]Institució Catalana de Recerca i Estudis Avançats (ICREA), Passeig Lluís Companys 23, 08010 Barcelona, Spain

ABSTRACT: A systematic study has been undertaken to determine how local distortions affect the overall (molecular) magnetic anisotropies in binuclear complexes. For this purpose we have applied a series of distortions to two binuclear Ni(II) model complexes and extracted the magnetic anisotropy parameters of multispin and giant-spin model Hamiltonians. Furthermore, local and molecular magnetic axes frames have been determined. It is shown that certain combinations of local distortions can lead to constructive interference of the local anisotropies and that the largest contribution to the anisotropic exchange does not arise from the second-rank tensor normally included in the multispin Hamiltonian, but rather from a fourth-rank tensor. From the comparison of the extracted parameters, simple rules are obtained to maximize the molecular anisotropy by controlling the local magnetic anisotropy, which opens the way to tune the anisotropy in binuclear or polynuclear complexes.

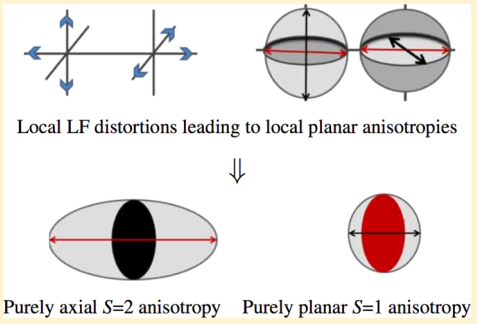

1. INTRODUCTION

Magnetic anisotropy is the origin of the single molecule magnet (SMM) behavior[1−5], which consists of a slow relaxation of the magnetization and a blocking of the magnetization for low enough temperatures. Since this bistable behavior may lead to technological applications in the domain of data storage[6] and quantum computing,[7−9] the understanding of the microscopic origin of magnetic anisotropy has received considerable interest during the last two decades. For most of the transition metal (TM) complexes, the property arises from the loss of degeneracy of the M_S components of the ground spin state S due to relativistic effects, in particular the spin−orbit coupling, combined with geometrical distortions from the highly symmetric octahedral or tetrahedral situations. This phenomenon is called the zero-field splitting (ZFS) and is characterized by the axial D and the rhombic E parameters. Magnetic anisotropy can also be observed in cases where the angular momentum is not quenched in the pure electronic ground state, due to for instance molecular orbital (near-)degeneracy in TM complexes, and lanthanide or actinide complexes. In such cases a pseudospin $\tilde{S}$ can be defined, which may significantly differ from the true spin state.[10]

For an even number of unpaired electrons, bistable behavior occurs when the complex has a uniaxial magnetic anisotropy and the two maximal $|M_S|$ components of the ground spin state are the lowest degenerate states, that is, when $E = 0$ and D is large and negative. In case of nonzero rhombic anisotropy ($E \neq 0$), the M_s^{min} and M_s^{max} components are coupled, and the ground state is a linear combination of M_S components. When D is positive, the lowest $|M_S|$ component becomes the dominant component of the ground state, and no bistability can be observed. In the case of an odd number of unpaired electrons, slow relaxation of the magnetization can *a priori* be observed even if the ground Kramers doublet is essentially composed of the lowest $|M_S|$ components (corresponding to a positive D value), and even if the rhombic parameter E does not vanish.[11] Nevertheless, such systems are not very common, and also for odd-electron systems negative D-values are central to SMM behavior. The synthesis of new objects with improved anisotropy characteristics rests on the ability to control the nature (uniaxial or in-plane) and the magnitude of the magnetic anisotropy. Several theoretical works have been devoted in the last years to the understanding of the chemical and geometrical factors that govern the magnetic anisotropy in mononuclear species.[12−17] Because of the numerous driving forces (configurations d^n, geometries, strength of the ligand field, etc.), the conclusions of these studies are quite often system-specific, but theory allows one to understand and accurately predict the magnetic anisotropy characteristics of mononuclear species. In polynuclear complexes, the situation is more complicated since additional factors are expected to come into play:

- The different ions in the complex are likely to have different local anisotropies. Indeed, the relativistic effects, responsible for the loss of degeneracy of the spin

Received: January 23, 2014
Published: April 23, 2014

 © 2014 American Chemical Society dx.doi.org/10.1021/ic500180k | *Inorg. Chem.* 2014, 53, 4508−4516

components of the ground spin state S_i of each ion i, are essentially local and hence very sensitive to the local environment of each ion, which may significantly differ from ion to ion.

- Intersite anisotropic interactions (such as the anisotropic exchange) may be present, affecting the characteristics of the overall magnetic anisotropy of the polynuclear complex, here called the molecular anisotropy.

The main aim of the present study is to advance the understanding of synergistic effects between local anisotropies. We consider model binuclear complexes constituted of two Ni(II) ions adopting various geometries for which both the nature and the magnitude of the local anisotropies may or may not be different. In all the cases considered, the parameters characterizing the local anisotropies are determined and confronted to those of the molecular magnetic anisotropy of the complex. Two types of anisotropic spin Hamiltonians can be used to characterize the ZFS of polynuclear complexes:

- The giant-spin Hamiltonian reproduces the energy levels of a single spin state, usually the ground spin state. Nevertheless several giant-spin Hamiltonians can be extracted to describe the energy levels of all the different spin states of a complex. When the molecular system contains four unpaired electrons or more ($S \geq 2$), and in particular in the weak-exchange limit, that is, when the mixing between the ground and the excited spin states is non-negligible, this model Hamiltonian contains spin operators of higher order than 2.
- The multispin Hamiltonian reproduces the energy of the M_S components of all spin states arising from the coupling between the local spin states of the paramagnetic ions. This Hamiltonian is spanned in the uncoupled $|S_a,M_{Sa},S_b,M_{Sb}\rangle$ basis and accounts for the spin mixing.

In recent studies, the physical content of these two Hamiltonians has been confronted to *ab initio* calculations based on the all-electron Hamiltonian.[18,19] It was shown that the usual approximations made in these models are not suitable to reproduce the interactions resulting from the *ab initio* calculations of a binuclear Ni(II) complex in the weak-exchange limit. In the case of the giant-spin Hamiltonian, simple additional operators were sufficient to consistently introduce the spin-mixing effect on the effective splitting and mixing of the M_S components of the ground spin state, and all non-negligible interactions could be extracted.[19] Concerning the multispin Hamiltonian, it was shown that a biquadratic operator and a four-rank tensor should be introduced to reproduce accurately all the effective non-negligible interactions arising from the all-electron Hamiltonian.[18] Unfortunately, the number of these interactions was too large, and a full extraction could not be performed. Owing to recent advances in our extraction procedure, such an extraction is now possible, and an important objective of the present work is to determine all non-negligible anisotropic interactions. Quite surprisingly, it will be shown that the fourth-rank tensor actually brings the main contributions to the exchange anisotropy.

It should be stressed that relations between the parameters of the local and molecular anisotropy tensors already exist[20−23] and that it is actually possible to determine the molecular magnetic anisotropy tensors by combining the local ones if the following two hypotheses are made: (i) the anisotropy axes on both magnetic centers are parallel, and (ii) the anisotropic intersite interactions of the two centers are negligible. The present Paper quantifies and discusses the various anisotropic interactions including those of the fourth-rank symmetric tensor from *ab initio* calculations, allowing us to determine the local and molecular anisotropies without the necessity of the mentioned assumptions.

The next section briefly presents the procedure of extraction of the model interactions from the effective Hamiltonian theory and provides the computational information. Section 3 recalls the physics of the two considered spin Hamiltonians and presents a method for the determination of the molecular and local magnetic axes frames. Section 4 discusses the magnitude and nature of the extracted local and molecular anisotropic interactions and analyzes interference effects between local anisotropies on the molecular anisotropy.

2. METHOD OF EXTRACTION AND COMPUTATIONAL INFORMATION

As shown in previous studies,[24−27] it is possible to establish the relevance of any model Hamiltonian and to extract its constitutive interactions by using the effective Hamiltonian theory. In combination with correlated *ab initio* calculations performed using the all-electron Hamiltonian, the effective Hamiltonian theory enables one to numerically evaluate all the matrix elements of a model Hamiltonian. This method has successfully been applied to mononuclear and binuclear systems to determine anisotropic interactions of the giant-spin and multispin Hamiltonians.[13,18,19,28−31]

The effective Hamiltonian theory[32,33] enables one to extract from accurate *ab initio* calculations the most rigorous effective Hamiltonian working in the same model space as the model Hamiltonian. This effective Hamiltonian is then compared to the model one. In the des Cloizeaux formalism,[33] the general expression of the effective Hamiltonian is

$$\hat{H}^{\text{eff}} = \sum_k |\tilde{\Psi}_k\rangle E_k \langle\tilde{\Psi}_k| \tag{1}$$

where $\tilde{\Psi}_k$ are the symmetrically orthogonalized and normalized projections onto the model space of the all-electron Hamiltonian eigenvectors Ψ_k, and E_k are the corresponding eigenvalues. This formulation ensures that the eigenvalues of the effective Hamiltonian are the energies of the all-electron Hamiltonian, while the eigenvectors of the effective Hamiltonian are the projections onto the model space of the all-electron Hamiltonian eigenvectors, such that

$$\hat{H}^{\text{eff}}|\tilde{\Psi}_k\rangle = E_k|\tilde{\Psi}_k\rangle \tag{2}$$

Since it is possible to calculate all the matrix elements of the effective Hamiltonian as

$$\langle i|\hat{H}^{\text{eff}}|j\rangle = \langle i|\sum_k |\tilde{\Psi}_k\rangle E_k \langle\tilde{\Psi}_k|j\rangle \tag{3}$$

the method provides more information than the low-energy spectrum. Values of the interactions of the model Hamiltonian can be assigned by confronting these numerical matrix elements to their analytical expression in the model Hamiltonian.

The *ab initio* calculations were performed using the Spin−Orbit State-Interaction (SO-SI) method[34,35] implemented in the MOLCAS package.[36,37] The method performs a variational treatment of the spin−orbit couplings between the lowest selected states. The preliminary spin−orbit free calculations

dx.doi.org/10.1021/ic500180k | Inorg. Chem. 2014, 53, 4508−4516

account for nondynamic correlation effects through the complete active space self-consistent field (CASSCF) method. The active space contains the 16 d electrons in the 10 d orbitals for the calculation of the magnetic anisotropy of the Ni(II) binuclear species, that is, CAS(16,10)SCF. To compute the local anisotropy tensors, the orbitals of each center were considered active alternatively while the orbitals of the other center were kept inactive; that is, CAS(8,5)SCF calculations were carried out. Extended basis sets of ANO type[38,39] were used with the following contractions: 6s5p4d2f for Ni, 6s5p2d for Cl, 4s3p1d for O and N, 3s2p for C, and 2s for H.

3. MODEL HAMILTONIANS AND THE MAGNETIC AXES FRAME

3.1. Giant-Spin Hamiltonians and Molecular Anisotropy Tensors. The simplest description of magnetic anisotropy in polynuclear systems is provided by the giant-spin approximation.[40−43] The use of this Hamiltonian is physically justified when the spin ground state of the molecule is sufficiently separated in energy from the other spin multiplets such that the magnetic properties can be described using a single spin ground state. Simultaneously, the ZFS of other spin multiplets can be independently described, which leads to a block-spin Hamiltonian if all the coupled spin states and the isotropic couplings are considered. In this work, we will focus in particular on the D and E parameters of the triplet and quintet states, referred to as D_1, E_1, D_2, and E_2, respectively.

The giant-spin Hamiltonian can be expressed in terms of the standard Stevens equivalent operators[44] and additional operators, which were shown to be necessary when $S = 2$ in the case of a binuclear complex in the weak-exchange limit.[19] Nevertheless, in case of a strong exchange coupling between the magnetic ions,[13] it can be reduced to its simple form:

$$\hat{H}_{GSH} = \hat{S}\overline{\overline{D}}\hat{S} \tag{4}$$

where $\hat{S}$ is the spin operator of the state under consideration, which in our case will be either the triplet ($S = 1$) or the quintet ($S = 2$) state for which the second-rank associated tensors will be denoted $\overline{\overline{D}}_1$ and $\overline{\overline{D}}_2$, respectively.

Higher than second-order terms become particularly significant when couplings between the different spin states (i.e., spin-mixing) are important but are small in the cases considered here since the isotropic magnetic coupling is relatively large (around 40 cm^{-1}); that is, we are in a situation close to the strong-exchange limit. The values of these interactions are not reported here since the largest value obtained is 0.09 cm^{-1}, affecting the $\langle 2, \pm 2|\hat{H}^{eff}|2, \mp 2\rangle$ matrix elements by not more than ∼1 cm^{-1}. The determination of the magnetic axes frame could therefore safely be performed using only the second-order tensors $S\cdot\overline{\overline{D}}_2\cdot S$ for the quintet state and $S\cdot\overline{\overline{D}}_1\cdot S$ for the triplet state (i.e., only the B_2^0 and B_2^2 parameters for both spin blocks are extracted, namely D_2, E_2, and D_1, E_1). For this purpose, we have artificially removed the couplings between the singlet, triplet, and quintet M_S components to extract the block spin anisotropy tensors and consequently diagonalize them to find the anisotropy axes, as proposed in a previous work.[19]

3.2. Multispin Hamiltonian. For a binuclear complex constituted of sites a and b, the multispin Hamiltonian works on the basis of the uncoupled $|M_{Sa},M_{Sb}\rangle$ functions. It is designed to reproduce the energy of all the states resulting from the coupling between the ground spin states of each magnetic site. In the present study, the Hamiltonian describes the energy of all M_S components of the singlet, triplet, and quintet states after transformation to the coupled $|S,M_S\rangle$ basis. As recently shown in a binuclear complex of Ni(II) in the weak-exchange limit, it involves biquadratic operators and a fourth-rank tensor $\overline{\overline{\overline{\overline{D}}}}_{aabb}$. In the considered case, its expression is

$$\begin{aligned}\hat{H}^{MS} = J\hat{S}_a\cdot\hat{S}_b + \hat{S}_a\overline{\overline{D}}_a\hat{S}_a + \hat{S}_b\overline{\overline{D}}_b\hat{S}_b + \hat{S}_a\overline{\overline{D}}_{ab}\hat{S}_b + \overline{d}_{ab}\hat{S}_a\times\hat{S}_b \\ + (\hat{S}_a\otimes\hat{S}_a)\overline{\overline{\overline{\overline{D}}}}_{aabb}(\hat{S}_b\otimes\hat{S}_b)\end{aligned} \tag{5}$$

where J is the isotropic magnetic exchange, $\overline{\overline{D}}_a$ and $\overline{\overline{D}}_b$ are local tensors, $\overline{\overline{D}}_{ab}$ is the symmetric anisotropic exchange tensor, and $\overline{d}_{ab}$ is the antisymmetric anisotropic term,[20−23] known as the Dzyaloshinskii−Moriya pseudovector. The components of these two tensors read as follows:

$$\begin{aligned}\overline{\overline{D}}_{ab} \quad + \quad \overline{d}_{ab} \\ = \begin{pmatrix} D^{xx} & D^{xy} & D^{xz} \\ D^{xy} & D^{yy} & D^{yz} \\ D^{xz} & D^{yz} & D^{zz} \end{pmatrix} + \begin{pmatrix} 0 & d^{xy} & -d^{xz} \\ -d^{xy} & 0 & d^{yz} \\ d^{xz} & -d^{yz} & 0 \end{pmatrix}\end{aligned} \tag{6}$$

Note that the analytical Hamiltonian matrix is given in reference 18 for centrosymmetric cases.

To compare the nature of the local and molecular anisotropies, the magnetic anisotropy axes were determined for each Ni(II) ions of the binuclear system in its triplet and quintet coupled spin states. For this purpose, the parameters of the various tensors of both Hamiltonians giant-spin and multispin were extracted from the effective Hamiltonian theory, such that the model Hamiltonian matrix calculated using the extracted values of the parameters reproduces at best the numerical effective Hamiltonian matrix calculated using eq 3.

Because the proper magnetic axes of each tensor may be different, all tensors are computed in a single axes frame and rotations ($P = R_z(\phi)\cdot R_x(\theta)\cdot R_z(\psi)$, where R_x and R_z stand for rotation around the x and z axes, respectively, and φ, θ, ψ are the Euler angles) between the proper axes frame of each tensor and the axes frame of the calculation are introduced, enabling one to determine the axial and rhombic parameters of all magnetic anisotropy tensors. Tables 1 and 2 give the number and nature of the nonzero parameters depending on the symmetry point group for the second-rank tensor $\overline{\overline{D}}_{ab}$, the Dzyaloshinski−Moriya vector, and the fourth-rank tensor. $\kappa = \pm 1$ indicates the absence/presence of a symmetry element that interchanges the two magnetic centers. To simplify the extraction, we have imposed the following relation

$$D^{xxxx} + D^{yyyy} + D^{zzzz} + 2D^{xxyy} + 2D^{xxzz} + 2D^{yyzz} = 0 \tag{7}$$

which has no other effect than ensuring that the anisotropic part of the Hamiltonian is traceless. To further reduce the number of independent variables, we make use of the fact that several matrix elements in the numerical effective Hamiltonian are (nearly) zero, whereas the corresponding elements of the model Hamiltonian is a (sum of) parameter(s). This introduces the following additional relations:

$$D^{xxxx} = D^{yyyy} = 0 \tag{8}$$

dx.doi.org/10.1021/ic500180k | Inorg. Chem. 2014, 53, 4508−4516

Table 1. Nonzero Symmetric and Antisymmetric Components of the Second-Rank Exchange Tensor[45]

point group[a]	κ[b]	symmetric components	antisymmetric components	number of independent components
C_1	+1	xx,yy,zz,xy,xz,yz	xy,xz,yz	9
C_i	−1	xx,yy,zz,xy,xz,yz		6
C_s[c]	−1	xx,yy,zz,xy	xz,yz	6
	+1		xy	5
C_2	−1	xx,yy,zz,xy	xz,yz	6
	+1		xy	5
D_2	−1	xx,yy,zz	xy	4
C_{2v}[d]	−1	xx,yy,zz	xz	4
	+1			3
C_{2h}	−1	xx,yy,zz,xy		4
D_{2h}	−1	xx,yy,zz		3
D_{2d}	−1	xx = yy,zz		2
C_n	+1	xx = yy,zz	xy	3
D_n	−1	xx = yy,zz	xy	3
C_{nv}	+1	xx = yy,zz		2
S_n,C_{nh}, D_{nh},D_{nd}	−1	xx = yy,zz		2

[a]The z-axis is the highest-order rotation axis. [b]$\kappa = -1$ if the magnetic centers are exchanged by a symmetry operation, and $\kappa = +1$ otherwise. [c]The σ_h plane is the xy plane. [d]The two magnetic centers are in the xz plane.

Table 2. Nonzero Symmetric Components of the Fourth-Rank $\overline{\overline{D}}_{aabb}$ Tensor

point group[a]	symmetric components	number of parameters[b]
C_2,C_s,C_{2h}	xxxx, yyyy, zzzz, xxyy, xxzz, yyzz & xyxy, xzxz, yyzz, xxxy, yyxy,zzxy	14
D_2,C_{2v},D_{2h}	xxxx, yyyy, zzzz, xxyy, xxzz,yyzz & xyxy, xzxz, yyzz	9
C_n,C_{nv},C_{nh},D_n,D_{nd},D_{nh}	xxxx = yyyy, zzzz,xxyy, xxzz = yyzz & xyxy, xzxz = yzyz	6

[a]The z-axis is the highest-order rotation axis. [b]Subject to reduction by additional relations (see text).

$$D^{xxyy} = \frac{1}{2}(D^{xxxx} - D^{xyxy}) \tag{9}$$

$$D^{xzxz} - D^{yzyz} = -D_{ab}^{xx} + D_{ab}^{yy} \tag{10}$$

$$D^{xxzz} - D^{yyzz} = 2D_{ab}^{xx} - 2D_{ab}^{yy} \tag{11}$$

For all cases studied here, there exists an appropriate axes frame for which the fourth-rank tensor reduces to at most nine independent components when these relations are imposed instead of the 81 possible *a priori*.

4. RESULTS AND DISCUSSION

Geometrical deformations were applied to the model complexes $O[Ni(NCH)_4CN]_2$ (M1, cases **1**, **10**, **11**, **13**; see Figure 1) and $O[Ni(NCH)_4Cl]_2$ (M2, cases **2**–**9**, and **12** see Figure 2) to tune the characteristics of the local and molecular anisotropies (see Figures 3–5 and Table 4). The stronger field exerted by the CN^- ligand makes it possible to study some extra combinations of local anisotropies that are not easily realized in the other complex, as specified below. Both model complexes show strong antiferromagnetic isotropic coupling and have an $S = 0$ ground state.

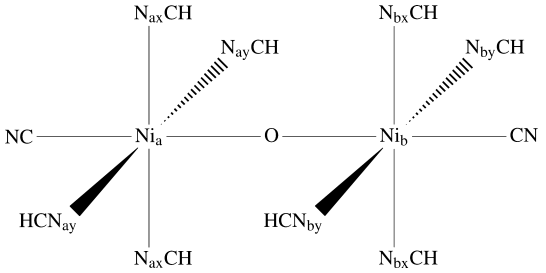

Figure 1. Scheme of the molecular model 1 (M1). Geometrical parameters: distances $l_{ax} = Ni_a–N_{ax}$, $l_{ay} = Ni_a–N_{ay}$, $l_{bx} = Ni_b–N_{bx}$, $l_{by} = Ni_b–N_{by}$, angles $\theta_a = (N_{ax},Ni_a,O)$, $\theta_b = (N_{bx},Ni_b,O)$ dihedral angles $\Phi_x = (N_{ax},Ni_a,Ni_b,N_{bx})$, $\Phi_y = (N_{ay},Ni_a,Ni_b,N_{by})$, $\Phi_{xy} = (N_{ax},Ni_a,Ni_b,N_{by})$.

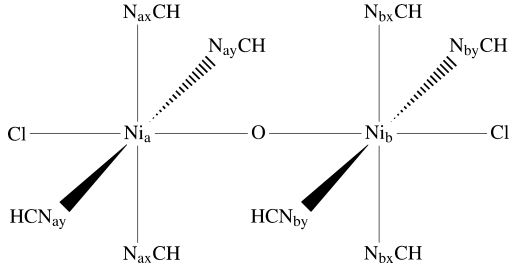

Figure 2. Scheme of the molecular model 2 (M2). Geometrical parameters: distances $l_{ax} = Ni_a–N_{ax}$, $l_{ay} = Ni_a–N_{ay}$, $l_{bx} = Ni_b–N_{bx}$, $l_{by} = Ni_b–N_{by}$, dihedral angles $\Phi_x = (N_{ax},Ni_a,Ni_b,N_{bx})$, $\Phi_y = (N_{ay},Ni_a,Ni_b,N_{by})$, $\Phi_{xy} = (N_{ax},Ni_a,Ni_b,N_{by})$.

For each structure, the parameters of three different models were extracted: (i) the local ZFS parameters D_a^{loc},E_a^{loc},D_b^{loc},E_b^{loc}, (ii) the giant-spin Hamiltonian parameters D_2,E_2 for the quintet and D_1,E_1 for the triplet spin manifolds, and (iii) all the parameters of the multispin Hamiltonian. The values are listed in Table 3. The proper magnetic axes of all the tensors were extracted and are represented in Figure 4 (both centers with axial local anisotropy), Figure 5 (both centers with planar local anisotropy), and Figure 6 (for axial and planar local anisotropies). These figures report pictures of the applied deformations and of the resulting anisotropy ellipsoids that provide a visualization of the nature of the magnetic anisotropies (both local and molecular for the quintet and triplet states); the direction of the Dzyaloshinskii–Moriya vector is also indicated when it is not zero. Note that the conventions used to represent the anisotropy in Figures 4–6 are given in Figure 3.

Compression, stretching, and angular distortion generate local anisotropies with peculiar and different features. The D_{4h} geometry (**5**) of $O[Ni(NCH)_4Cl]_2$ is such that Z is a hard axis of magnetization for both centers, and they do not exhibit any local rhombicity. In the D_{2h} structures (**6** and **2**) the bonds have been stretched or compressed in a single direction to generate either two parallel easy planes (Table 5) or two collinear easy axes (Table 4) of magnetization. In the D_{2d} structures (**7** and **3**), the deformations are applied to different axes (X and Y) such that the easy planes or the easy axes are orthogonal. Angular distortions (of 10 degrees on each site) were applied to both D_{2h} geometries to generate the D_2 structure in which the local easy planes (**8**) are no longer parallel. The C_{2v} (**9**) geometry illustrates the cases of two local planar anisotropies, where only one of them is rhombic. In the C_{2v} (**12**) geometry, one center has a planar anisotropy while the other has an axial anisotropy and the easy axis is parallel to the easy plane. Finally,

dx.doi.org/10.1021/ic500180k | Inorg. Chem. 2014, 53, 4508–4516

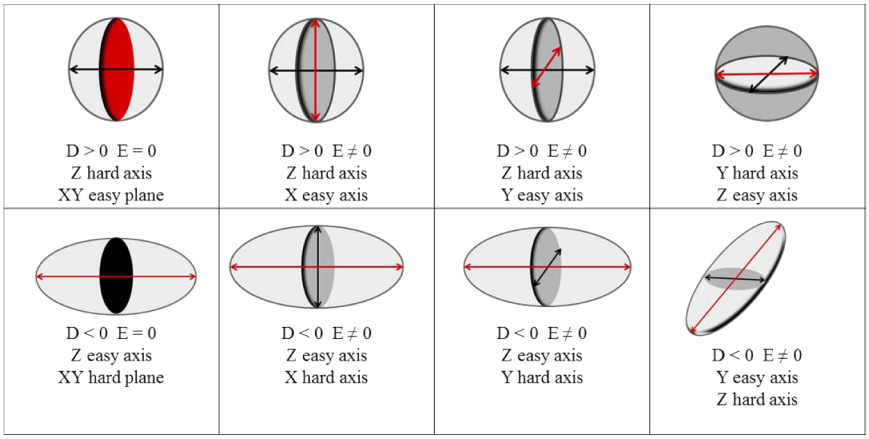

Figure 3. Conventions used to schematize the nature of the magnetic anisotropy and to show the magnetic axes frame of the D-tensors. A prolate ellipsoid indicates an axial anisotropy, while an oblate ellipsoid refers to a planar anisotropy. Hard axes and hard planes are represented in black, while easy axes and easy planes are in red. In absence of rhombicity only one axis is represented.

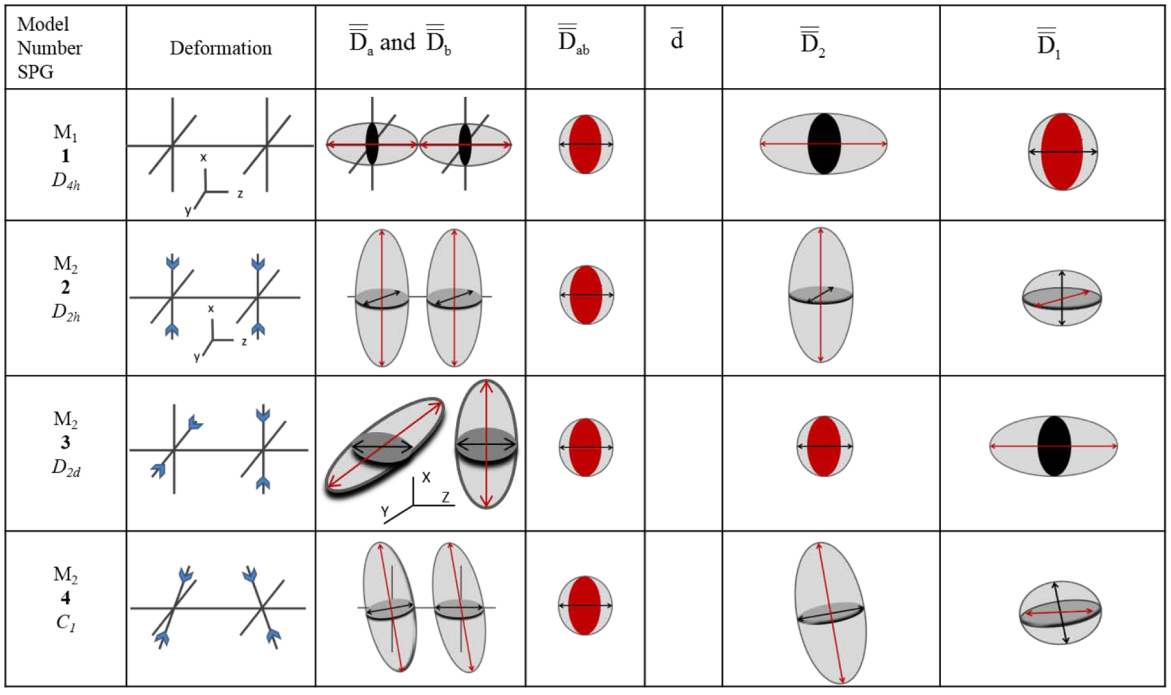

Figure 4. Ellipsoids representing the axial or planar anisotropy and magnetic anisotropy axes of the various local and molecular anisotropy tensors for different geometries in which local axial anisotropies have been imposed. The compound number and the model compound (either M1 or M2) are indicated in the left column.

in the C_1 structure (**4**) the two local anisotropies are axial; one of the easy axes is in the XY plane, and the other is in the XZ plane.

The ligand CN^- produces a stronger ligand field than the NCH one, which permits the study of other combinations of local anisotropies. In the D_{4h} structure (**1**) of O[Ni-$(NCH)_4CN]_2$, the local axial anisotropies share the same easy axis Z. The C_{4v} structure (**11**) has one axial local anisotropy with the easy axis Z and a local planar anisotropy with the easy plane XY. In the C_{2v} structure (**13**), one center has an axial anisotropy with the easy axis Z, while the other has a planar anisotropy with the easy plane YZ.

From the comparison of the values of the different local and molecular anisotropy parameters, a series of conclusions can be extracted, which will be discussed below in a point-by-point fashion.

- The magnetic axes frames and local anisotropy parameters extracted from the calculations performed with one or two active magnetic centers are very similar, showing the transferability of these parameters from the "embedded" monomer to the dimer. The small discrepancies are due to the bias introduced in the calculations of the local tensors by the arbitrarily imposed closed-shell character of the inactive Ni(II) center. The values of the local anisotropy parameters that should be considered as the most precise are those extracted from the calculations in which the two magnetic centers are active.
- The values of D_{ab} and E_{ab} (anisotropic exchange parameters) are very small and slightly more important when the local anisotropy is planar rather than axial. The anisotropy of the interaction between the two anisotropic

dx.doi.org/10.1021/ic500180k | Inorg. Chem. 2014, 53, 4508−4516

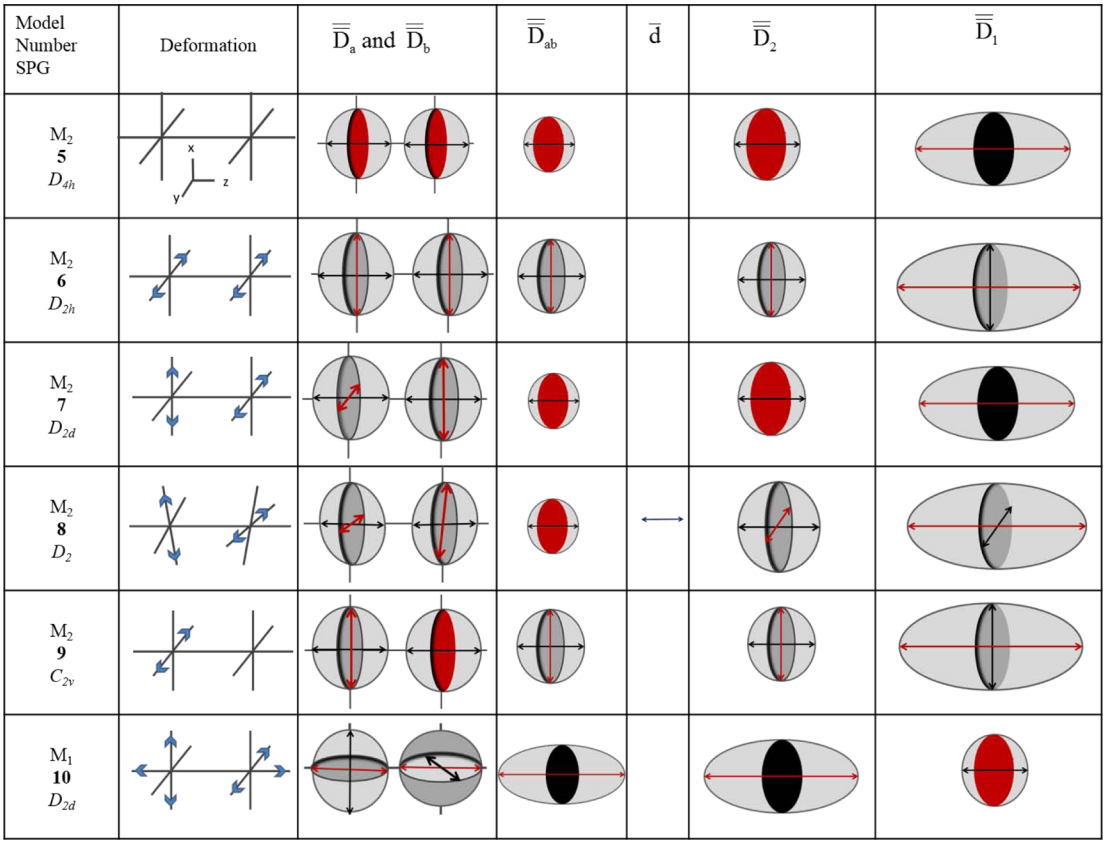

Figure 5. Ellipsoids representing the axial or planar anisotropy and magnetic anisotropy axes of the various local and molecular anisotropy tensors for different geometries in which local planar anisotropies have been imposed. The compound number and the model compound (either M1 or M2) are indicated in the left column.

Table 3. Values of Extracted Parameters in cm^{-1}

cases	1	2	3	4	5	6	7	8	9	10	11	12	13
SPG	D_{4h}	D_{2h}	D_{2d}	C_1	D_{4h}	D_{2h}	D_{2d}	D_2	C_{2v}	D_{2d}	C_{4v}	C_{2v}	C_{2v}
D_a^{loc}[a]	−3.1	−21.9	−19.4	−22.5	10.0	9.9	10.0	8.5	9.9	15.0	−4.3	2.2	−3.8
D_b^{loc}	−3.1	−21.9	−19.4	−24.4	10.0	9.9	10.0	8.5	9.6	15.0	2.1	−21.7	5.4
E_a^{loc}	0[b]	3.7	2.8	0.6	0	1.6	1.5	1.8	1.5	1.3	0	0.1	1.1
E_b^{loc}	0	3.7	2.8	0.1	0	1.6	1.5	1.8	0.0[b]	1.3	0	2.6	0.0
D_2	−2.4	−6.7	2.5	−6.6	2.5	2.5	2.5	1.6	2.5	−2.2	−1.5	−3.6	−2.5
E_2	0	0.7	0	0.6	0	0.5	0	0.2	0.2	0	0	0.2	0.3
D_1	7.6	19.2	−6.9	18.6	−6.6	−6.7	−6.6	−3.7	−6.7	9.7	5.2	8.6	8.0
E_1	0	2.3	0	2.4	0	1.4	0	0.5	0.7	0	0	1.4	0.9
J	38.9	50.3	49.7	49.8	40.9	41.1	41.1	41.0	41.8	30.6	40.3	38.6	37.2
D_a	−2.2	−21.1	−21.9	−20.7	10.9	12.0	12.1	9.3	12.0	16.6	−3.6	4.6	−2.1
D_b	−2.2	−21.1	−21.9	−21.3	10.9	12.0	12.1	9.3	12.0	16.6	1.1	−20.3	4.2
E_a	0	0.4	0.3	0.6	0	1.4	1.4	1.4	1.4	3.1	0	0.0	0.0
E_b	0	0.4	0.3	0.1	0	1.4	1.4	1.4	0.0	3.1	0	0.9	0.5
D_{ab}	0.3	0.3	0.3	0.3	0.4	5.2	0.4	0.4	5.1	−4.7	0.3	0.3	−4.7
E_{ab}	0	0.0	0	0.0	0	0.9	0	0.0	0.5	0	0	0.0	0.6
D_{zzzz}	−4.9	−4.0	−5.4	−3.6	−3.8	−4.8	−4.9	−4.9	−4.9	5.5	−3.6	−3.0	−5.4
D_{xxzz}	0	0	0	0	0	−1.3	0	0	−2.2	3.3	0	0	2.2
D_{yyzz}	0	0	0	0	0	−5.0	0	0	−4.1	3.3	0	0	4.7
D_{xxyy}	2.5	2.0	2.7	1.8	1.9	8.7	2.4	2.4	8.7	−9.4	1.8	1.5	−4.2
D_{xyxy}	−1.2	−1.0	−1.4	−0.9	−0.9	−4.4	−1.2	−1.2	4.4	4.7	−0.9	−0.7	2.1
D_{xzxz}	−1.3	−1.1	−1.4	−1.3	0	−0.6	−1.2	−1.3	−0.1	−0.3	−0.9	−0.8	−2.4
D_{yzyz}	−1.3	−1.0	−1.4	−1.3	0	1.3	−1.2	−1.3	0.8	−0.3	−0.9	−0.8	−3.6

[a]The values of the local tensors components marked with a superscripted "loc" have been extracted from calculations performed with a single magnetic active center. [b]Note that "0" is used for terms that are strictly zero for symmetry reasons, while "0.0" indicates that the extracted value of the parameter is smaller than 0.05 cm^{-1}.

dx.doi.org/10.1021/ic500180k | Inorg. Chem. 2014, 53, 4508−4516

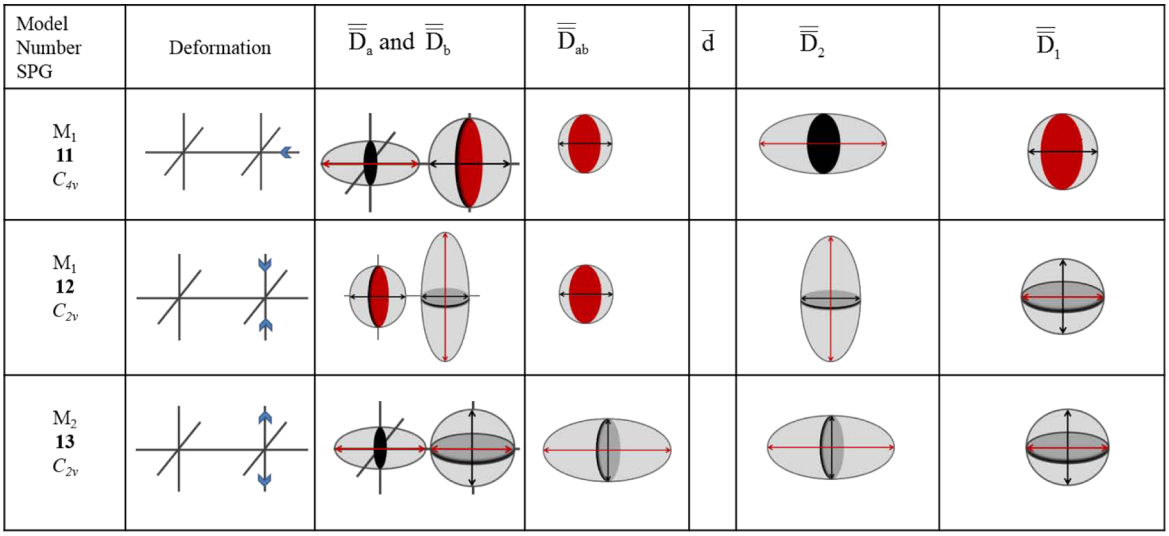

Figure 6. Ellipsoids representing the axial or planar anisotropy and magnetic anisotropy axes of the various local and molecular anisotropy tensors for different geometries in which both an axial and a planar local anisotropies have been imposed. The compound number and the model compound (either M1 or M2) are indicated in the left column.

centers originates essentially in the fourth-rank tensor components. The planar nature of the anisotropy caused by $\overline{\overline{D}}_{ab}$ appears to be almost unaffected by the distortions in the considered systems, except for cases **10** and **13**.

- The giant-spin second-rank tensors $\overline{\overline{D}}_1$ and $\overline{\overline{D}}_2$ exhibit opposite anisotropic characteristics; the axes and planes of easy and hard magnetization are systematically opposite. For simplicity, only the values and features of $\overline{\overline{D}}_2$ will be commented on in the subsequent points. One may also note that the absolute values of the anisotropy parameters are larger in the triplet ($\overline{\overline{D}}_1$) than they are in the quintet ($\overline{\overline{D}}_2$), as already explained by Boča.[22] Because of the presence of the fourth-rank tensor in the model Hamiltonian considered in this work, and in some cases due to the mismatch between the local tensor anisotropy axes, the relations between the tensors found in this study are different than those proposed earlier.[22]
- As expected, stretching and compression induce opposite local anisotropy behavior with planar and axial anisotropy, respectively. This results in positive and negative D_2 values.
- The Dzyaloshinskii−Moriya vector is either very small or strictly zero by symmetry. Among the considered cases, nonzero values were only found for the C_{2v} and C_1 symmetry point groups. Since the obtained values were lower than 0.05 cm^{-1}, they have not been reported here.
- When both local anisotropies are axial (see Figure 4), the nature of the anisotropy of the quintet is usually axial except when the two local axes are orthogonal (case **3**). The easy axis always bisects the two local easy axes (and is therefore parallel or collinear—i.e., parallel and having a common point—with the local axes when these ones are already parallel or collinear). Note that the values of the molecular anisotropy parameters are usually drastically reduced in comparison to the local ones. The most interesting situation (case **1**) occurs when the local axes are collinear, as expected. Note that in such a case the absence of local rhombicity is maintained in the molecular magnetic anisotropy of the complex and that there is a (small) synergistic effect: the overall magnetic axial parameter value for the high-spin block is −2.4 cm^{-1}, while the local ones are −2.2 cm^{-1}.
- When both local anisotropies are planar (see Figure 5), the molecular magnetic anisotropy is usually planar, and here again the values of the anisotropic parameters are smaller than the local ones. Introducing local rhombicity may actually be interesting for tuning the nature of the overall anisotropy of the complex. Indeed, if the local planes are parallel and the local easy axes are perpendicular, the overall magnetic anisotropy does not exhibit any rhombicity (case 7). When the local easy axes have an angle, the resulting easy axis bisects the two local ones (cases **6** and **8**). The most interesting situation occurs when the local easy planes are orthogonal and the local easy axes are collinear, since it is possible to generate a purely axial anisotropy (negative axial parameter and no rhombicity).
- When the nature of the local anisotropies is different (one axial and one planar, cases **11**−**13**; see Figure 6), it is possible to generate an axial molecular magnetic anisotropy independent of the orientation of the local easy axis and plane (cases **11** and **12**). Two interesting situations should be noted: (i) the absence of local rhombicities (case **11**) leads to the absence of rhombic molecular magnetic anisotropy, and (ii) a synergistic effect occurs when the local easy axes are collinear as in case **13**, where the local axial parameter D_a is −2.1 cm^{-1}, while the overall axial parameter D_2 is −2.5 cm^{-1}.

5. SUMMARY AND PERSPECTIVES

This work is a follow-up of previous theoretical studies in which it was shown that both the commonly applied giant-spin and multispin Hamiltonians are not appropriate for the description of the anisotropy of binuclear complexes, in particular in the weak-exchange limit.[18,19] Because the values of the numerous parameters of the multispin Hamiltonian involving the fourth-rank tensor components could not be extracted up to now,[18] a method of extraction that makes use of the effective Hamiltonian theory was implemented here and successfully

dx.doi.org/10.1021/ic500180k | Inorg. Chem. 2014, 53, 4508−4516

applied to complexes exhibiting different local anisotropies. Rules to predict vanishing values of symmetric and antisymmetric second-rank exchange tensors and symmetric fourth-rank symmetric tensors were presented, illustrated (see Figures 4−6), and tested on model molecules.

Several conclusions can be drawn from this work. Among the most important ones, one should mention that the anisotropy of the interactions between the two magnetic centers is essentially caused by the symmetric fourth-rank tensor, while the second-rank exchange tensor components are almost always negligible. As a consequence, the relations between the molecular anisotropy of the complex and the local ones are no more quantitatively valid. Nevertheless, from a qualitative point of view the nature of the overall magnetic anisotropy can be anticipated from the local anisotropy, except when the complex belongs to the weak-exchange regime. Also note that the Dzyaloshinskii−Moriya term is very small in the considered cases and that nonzero values were only obtained for symmetry point groups lower than C_{2v}. Obtaining larger antisymmetric terms would require other deformations, such as changing the (Ni_a,O,Ni_b) angle away from 180°.

Combinations of local anisotropies were found to show synergistic effects (increased axiality of the molecular magnetic anisotropy in comparison to the local ones) in three cases. The first one occurs when two local axial anisotropies with collinear local easy axes are combined. The molecular axial anisotropy is larger than the sum of the local anisotropies. This is in line with the results of experimentalists working in the domain of polynuclear single-molecule or single-chain magnets for instance.[46] The second case of synergy is observed when two local planar, rhombic anisotropies are combined, leading to a purely axial (no rhombicity) molecular anisotropy when the local easy axes are collinear and the local easy planes are perpendicular. Finally, axial and planar local anisotropies may lead to an axial molecular anisotropy, and a synergy occurs when the local easy axis of one center is in the local easy plane of the other center.

To the best of our knowledge, values of the multispin parameters are extremely difficult to extract from experiment. In this respect, a theoretical approach that provides both qualitative and quantitative information concerning magnetic anisotropy appears as an interesting means to help synthetic chemists control and improve this property. Forthcoming papers will be devoted to the application of the here-presented method of extraction to existing, synthesized compounds.

AUTHOR INFORMATION

Corresponding Author

*E-mail: nathalie.guihery@irsamc.ups-tlse.fr.

Notes

The authors declare no competing financial interest.

ACKNOWLEDGMENTS

Financial support was provided by the Spanish administration (Project CTQ2011-23140) and the Generalitat de Catalunya (Project 2009SGR462 and *Xarxa d'R+D+I en Química Teòrica i Computacional*, XRQTC). This work was supported by the French Centre National de la Recherche Scientifique (CNRS), by the Université de Toulouse, and by the Agence Nationale de la Recherche (ANR) (Project TEMAMA ANR-09-BLAN-0195-01).

REFERENCES

(1) Sessoli, R.; Tsai, H. L.; Schake, A. R.; Wang, S.; Vincent, J. B.; Folting, K.; Gatteschi, D.; Christou, G.; Hendrickson, D. N. *J. Am. Chem. Soc.* **1993**, *115*, 1804−1816.

(2) Sessoli, R.; Gatteschi, D.; Caneschi, M. A.; Novak, A. *Nature* **1993**, *365*, 141−143.

(3) Gatteschi, D.; Sessoli, R.; Villain, J. *Molecular Nanomagnets;* Oxford University Press: New York, 2006.

(4) Milios, C. J.; Vinslava, A.; Wernsdorfer, W.; Moggach, S.; Parsons, S.; Perlepes, S. P.; Christou, G.; Brechin, E. K. *J. Am. Chem. Soc.* **2007**, *129*, 2754−2755.

(5) Yoshihara, D.; Karasawa, S.; Koga, N. *J. Am. Chem. Soc.* **2008**, *130*, 10460−10461.

(6) Mannini, M.; Pineider, F.; Sainctavit, P.; Danieli, C.; Otero, E.; Sciancalepore, C.; Talarico, A.; Arrio, M.-A.; Cornia, A.; Gatteschi, D.; Sessoli, R. *Nat. Mater.* **2009**, *8*, 194−197.

(7) Leuenberger, M. N.; Loss, D. *Nature* **2001**, *410*, 789−793.

(8) Ardavan, A.; Rival, O.; Morton, J. J. L.; Blundell, S. J.; Tyryshkin, A. M.; Timco, G. A.; Winpenny, R. E. P. *Phys. Rev. Lett.* **2007**, *98*, 057201.

(9) Stamp, P. C. E.; Gaita-Arino, A. *J. Mater. Chem.* **2009**, *19*, 1718−1730.

(10) Chibotaru, L. F.; Ungur, L. *J. Chem. Phys.* **2012**, *137*, 064112.

(11) Zadrozny, J. M.; Liu, J.; Piro, N. A.; Chang, C. J.; Hill, S.; Long, J. R. *Chem. Commun.* **2012**, *48*, 3927−3929.

(12) Cirera, J.; Ruiz, E.; Alvarez, S.; Neese, F.; Kortus, J. *Chem.—Eur. J.* **2009**, *15*, 4078−4087.

(13) Maurice, R.; de Graaf, C.; Guihéry, N. *J. Chem. Phys.* **2010**, *133*, 084307.

(14) Atanasov, M.; Ganyushin, D.; Pantazis, D. A.; Sivalingam, K.; Neese, F. *Inorg. Chem.* **2011**, *50*, 7460−7477.

(15) McGarvey, B.; Telser, J. *Inorg. Chem.* **2012**, *51*, 6000−6010.

(16) Ruamps, R.; Maurice, R.; Batchelor, L. J.; Boggio-Pasqua, M.; Guillot, R.; Barra, A.-L.; Liu, J.; Bendeif, E.-E.; Pillet, S.; Hill, S.; Mallah, T.; Guihéry, N. *J. Am. Chem. Soc.* **2013**, *135*, 3017−3026.

(17) Gomez-Coca, S.; Cremades, E.; Aliaga-Alcalde, N.; Ruiz, E. *J. Am. Chem. Soc.* **2013**, *135*, 7010−7018.

(18) Maurice, R.; Guihéry, N.; Bastardis, R.; de Graaf, C. *J. Chem. Theory Comput.* **2010**, *6*, 55−65.

(19) Maurice, R.; de Graaf, C.; Guihéry, N. *Phys. Rev. B* **2010**, *81*, 214427.

(20) Kahn, O. *Molecular Magnetism;* VCH Publishers: Weinheim, Germany, 1993.

(21) Boča, R. *Theoretical Foundations of Molecular Magnetism;* Elsevier: Amsterdam, 1999.

(22) Boča, R. *Coord. Chem. Rev.* **2004**, *248*, 757−815.

(23) Boča, R.; Herchel, R. *Coord. Chem. Rev.* **2010**, *254*, 2973−3025.

(24) Calzado, C. J.; Cabrero, J.; Malrieu, J.-P.; Caballol, R. *J. Chem. Phys.* **2002**, *116*, 2728−2747.

(25) Calzado, C. J.; Cabrero, J.; Malrieu, J.-P.; Caballol, R. *J. Chem. Phys.* **2002**, *116*, 3985−4000.

(26) Bastardis, R.; Guihéry, N.; de Graaf, C. *J. Chem. Phys.* **2008**, *129*, 104102.

(27) Malrieu, J.-P.; Caballol, R.; Calzado, C. J.; de Graaf, C.; Guihéry, N. *Chem. Rev.* **2014**, *114*, 429−492.

(28) Maurice, R.; Bastardis, R.; de Graaf, C.; Suaud, N.; Mallah, T.; Guihéry, N. *J. Chem. Theory Comput.* **2009**, *5*, 2977−2984.

(29) Maurice, R.; Pradipto, A. M.; Guihéry, N.; Broer, R.; de Graaf, C. *J. Chem. Theory Comput.* **2010**, *6*, 3092−3101.

(30) Ruamps, R.; Batchelor, L. J.; Maurice, R.; Gogoi, N.; Jiménez-Lozano, P.; Guihéry, N.; de Graaf, C.; Barra, A.-L.; Sutter, J.-P.; Mallah, T. *Chem.—Eur. J.* **2013**, *19*, 950−956.

(31) Maurice, R.; Verma, P.; Zadrozny, J. M.; Luo, S.; Borycz, J.; Long, J. R.; Truhlar, D. G.; Gagliardi, L. *Inorg. Chem.* **2013**, *52*, 9379−9389.

(32) Bloch, C. *Nucl. Phys.* **1958**, *6*, 329−347.

(33) des Cloizeaux, J. *Nucl. Phys.* **1960**, *20*, 321−346.

(34) Malmqvist, P.-Å.; Roos, B. O.; Schimmelpfennig, B. *Chem. Phys. Lett.* **2002**, *357*, 230−240.

(35) Roos, B. O.; Malmqvist, P.-Å. *Phys. Chem. Chem. Phys.* **2004**, *6*, 2919−2927.
(36) Karlström, G.; Lindh, R.; Malmqvist, P.-Å.; Roos, B. O.; Ryde, U.; Veryazov, V.; Widmark, P.-O.; Cossi, M.; Schimmelpfennig, B.; Neogrady, P.; Seijo, L. *Comput. Mater. Sci.* **2003**, *28*, 222−239.
(37) Aquilante, F.; De Vico, L.; Ferré, N.; Ghigo, G.; Malmqvist, P.-A.; Neogrády, P.; Pedersen, T. B.; Pitonák, M.; Reiher, M.; Roos, B. O.; Serrano-Andrés, L.; Urban, M.; Veryazov, V.; Lindh, R. *J. Comput. Chem.* **2010**, *31*, 224−247.
(38) Roos, B. O.; Lindh, R.; Malmqvist, P.-Å.; Veryazov, V.; Widmark, P.-O. *J. Phys. Chem. A* **2004**, *108*, 2851−2858.
(39) Roos, B. O.; Lindh, R.; Malmqvist, P.-Å.; Veryazov, V.; Widmark, P.-O. *J. Phys. Chem. A* **2005**, *109*, 6575−6579.
(40) Gatteschi, D.; Sessoli, R. *Angew. Chem., Int. Ed.* **2003**, *42*, 268−297.
(41) Barra, A. L.; Gatteschi, D.; Sessoli, R. *Phys. Rev. B* **1997**, *56*, 8192−8198.
(42) Hill, S.; Perenboom, J. A. A. J.; Dalal, N. S.; Hathaway, T.; Stalcup, T.; Brooks, J. S. *Phys. Rev. Lett.* **1998**, *80*, 2453−2456.
(43) Wilson, A.; Lawrence, J.; Yang, E.-C.; Nakano, M.; Hendrickson, D. N.; Hill, S. *Phys. Rev. B* **2006**, *74*, 140403.
(44) Abragam, A.; Bleaney, B. *Electron Paramagnetic Resonance of Transition Ions;* Dover Publications: Dover, NY, 1986.
(45) Buckingham, A. D.; Pyykko, P.; Robert, J. B.; Wiesenfeld, L. *Mol. Phys.* **1982**, *46*, 177−182.
(46) Gogoi, N.; Thlijeni, M.; Duhayon, C.; Sutter, J.-P. *Inorg. Chem.* **2013**, *52*, 2283−2285.